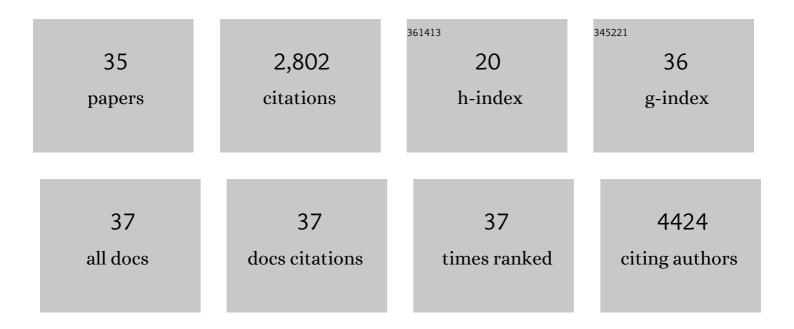
Seoung Ho Lee

List of Publications by Year in descending order

Source: https://exaly.com/author-pdf/309614/publications.pdf Version: 2024-02-01



#	Article	IF	CITATIONS
1	Highly Conductive PEDOT:PSS Nanofibrils Induced by Solutionâ€Processed Crystallization. Advanced Materials, 2014, 26, 2268-2272.	21.0	856
2	An Excimer-Based, Binuclear, Onâ^Off Switchable Calix[4]crown Chemosensor. Journal of the American Chemical Society, 2004, 126, 16499-16506.	13.7	303
3	Efficient planar-heterojunction perovskite solar cells achieved via interfacial modification of a sol–gel ZnO electron collection layer. Journal of Materials Chemistry A, 2014, 2, 17291-17296.	10.3	274
4	Highly Conductive Allâ€Plastic Electrodes Fabricated Using a Novel Chemically Controlled Transferâ€Printing Method. Advanced Materials, 2015, 27, 2317-2323.	21.0	239
5	Controlling Molecular Ordering in Aqueous Conducting Polymers Using Ionic Liquids. Advanced Materials, 2016, 28, 8625-8631.	21.0	149
6	Molecular Taekwondo. 2. A New Calix[4]azacrown Bearing Two Different Binding Sites as a New Fluorescent Ionophore. Journal of Organic Chemistry, 2003, 68, 597-600.	3.2	130
7	Indium(III)-Induced Fluorescent Excimer Formation and Extinction in Calix[4]areneâ [^] Fluoroionophores. Inorganic Chemistry, 2005, 44, 7866-7875.	4.0	103
8	UV Band Splitting of Chromogenic Azo-Coupled Calix[4]crown upon Cation Complexation. Journal of Organic Chemistry, 2003, 68, 1933-1937.	3.2	73
9	Regioselective Complexation of Metal Ion in Chromogenic Calix[4]biscrowns. Journal of Organic Chemistry, 2004, 69, 2902-2905.	3.2	69
10	Broad Workâ€Function Tunability of pâ€Type Conjugated Polyelectrolytes for Efficient Organic Solar Cells. Advanced Energy Materials, 2015, 5, 1401653.	19.5	59
11	Pyrene-appended calix[4]crowned logic gates involving normal and reverse PET: NOR, XNOR and INHIBIT. Tetrahedron, 2004, 60, 5171-5176.	1.9	56
12	Silver Ion Shuttling in the Trimer-Mimic Thiacalix[4]crown Tube. Journal of Organic Chemistry, 2004, 69, 2877-2880.	3.2	52
13	Calix[4]crown in dual sensing functions with FRET. Tetrahedron Letters, 2005, 46, 8163-8167.	1.4	47
14	Potassium ion-selective membrane electrodes based on 1,3-alternate calix[4]crown-5-azacrown-5. Talanta, 2003, 61, 709-716.	5.5	39
15	Radical Cation–Anion Couplingâ€Induced Work Function Tunability in Anionic Conjugated Polyelectrolytes. Advanced Energy Materials, 2015, 5, 1501292.	19.5	39
16	Water-Soluble Conjugated Polyelectrolytes with Branched Polyionic Side Chains. Macromolecules, 2011, 44, 4742-4751.	4.8	38
17	Variable-Band-Gap Poly(arylene ethynylene) Conjugated Polyelectrolytes Adsorbed on Nanocrystalline TiO ₂ : Photocurrent Efficiency as a Function of the Band Gap. ACS Applied Materials & Interfaces, 2009, 1, 381-387.	8.0	35
18	Long-Term Stable Recombination Layer for Tandem Polymer Solar Cells Using Self-Doped Conducting Polymers. ACS Applied Materials & Interfaces, 2016, 8, 6144-6151.	8.0	34

SEOUNG HO LEE

#	Article	IF	CITATIONS
19	Role of the Side Chain in the Phase Segregation of Polymer:Fullerene Bulk Heterojunction Composites. Advanced Energy Materials, 2013, 3, 1575-1580.	19.5	25
20	Conjugated Polyelectrolyte Dendrimers: Aggregation, Photophysics, and Amplified Quenching. Langmuir, 2012, 28, 16679-16691.	3.5	22
21	A Sensitive and Selective Mercury(II) Sensor Based on Amplified Fluorescence Quenching in a Conjugated Polyelectrolyte/Spiro yclic Rhodamine System. Macromolecular Rapid Communications, 2013, 34, 791-795.	3.9	20
22	A Color Version of the Hinsberg Test: 1°–3° Amine Indicator. Chemistry - A European Journal, 2007, 13, 3082-3088.	3.3	18
23	Optimized phase separation in low-bandgap polymer:fullerene bulk heterojunction solar cells with criteria of solvent additives. Nano Energy, 2016, 30, 200-207.	16.0	18
24	Self-assembly of pyrene boronic acid-based chemodosimeters for highly efficient mercury(II) ion detection. Tetrahedron Letters, 2019, 60, 151048.	1.4	15
25	Interfacial Morphology and Photoelectrochemistry of Conjugated Polyelectrolytes Adsorbed on Single Crystal TiO ₂ . Langmuir, 2011, 27, 11906-11916.	3.5	11
26	Micellization-induced amplified fluorescence response for highly sensitive detection of heparin in serum. Scientific Reports, 2020, 10, 9438.	3.3	11
27	A micellized fluorescence sensor based on amplified quenching for highly sensitive detection of non-transferrin-bound iron in serum. Dalton Transactions, 2020, 49, 4660-4664.	3.3	9
28	Optimization of graphene oxide synthesis parameters for improving their after-reduction material performance in functional electrodes. Materials Research Express, 2016, 3, 105033.	1.6	8
29	A ratiometric fluorescence sensor based on enzymatically activatable micellization of TPE derivatives for quantitative detection of alkaline phosphatase activity in serum. RSC Advances, 2020, 10, 26888-26894.	3.6	8
30	"Light Switch―Effect Upon Binding of Ru-dppz to Water-Soluble Conjugated Polyelectrolyte Dendrimers. Journal of Physical Chemistry Letters, 2012, 3, 1707-1710.	4.6	5
31	A self-assembled conjugated micelle with improved sensitivity for monitoring alkaline phosphatase activity. Tetrahedron Letters, 2019, 60, 2022-2025.	1.4	5
32	Pyridine-Chelated Imidazo[1,5-a]Pyridine N-Heterocyclic Carbene Nickel(II) Complexes for Acrylate Synthesis from Ethylene and CO2. Catalysts, 2020, 10, 758.	3.5	5
33	Energy Transfer in Extended Thienylene-Phenylene-Ethynylene Dendrimers. Journal of Physical Chemistry B, 2011, 115, 15214-15220.	2.6	4
34	Effect of Bulky Atom Substitution on Backbone Coplanarity and Electrical Properties of Cyclopentadithiopheneâ€Based Semiconducting Polymers. Macromolecular Rapid Communications, 2022, 43, e2100709.	3.9	2
35	Efficient Imidazoliumâ€Biomolecule Interactionâ€Assisted Amplified Quenching for Ultrasensitive Detection of Heparin. Chemistry - an Asian Journal, 0, , .	3.3	0